

AUTOMATIZATED PROCESSING FOR PHOTOELASTIC PARAMETERS

Gualter Aurélio Alves de Souza

Federal University of Uberlândia, School of Mechanical Engineering. Av. João Naves de Ávila, 2121 – Bl. 1M, Uberlândia, Minas Gerais, CEP: 38400-089, Brazil
gualter@mecanica.ufu.br

Cleudmar Amaral de Araújo

Federal University of Uberlândia, School of Mechanical Engineering. Av. João Naves de Ávila, 2121 – Bl. 1M, Uberlândia, Minas Gerais, CEP: 38400-089, Brazil
cleudmar@mecanica.ufu.br

Abstract. Photoelasticity is an experimental technique used for getting solution for complex engineering problems, specially when analytical and numeric solution is difficult to apply. Photoelasticity is also used for study the stress distribution when the geometry or load distribution is complex. One of the difficulties for the application of this technique is that the photoelastic parameters are obtained by direct reading. The direct reading depends on large experience and demands a variable time for analysis and solution. The main objective of this work is to develop a software that gets the photoelastic parameter by an automatized process. This method uses elliptical polarized light and a calibration model for fringe order analysis. The photoelastic model images are digitalized and treated by the software. The model images are got by use of the elliptical polarized light, and the directions of the principal stress are obtained. To validate this technique, a disc is loaded by compression. The analysis of the fringe order is possible by using a calibration model made of the same material of the disc. This calibration model is loaded by pure bending, wich has rectangular cross section, and was used for the generation of the RGB values for the different fringe orders.

Keywords: *Photoelasticity, stress, experimental analysis, Photoelastic images, Photoelastic parameters.*

1. Introduction

Presently, the mechanical systems design involves two basic steps of development: theoretical analysis and experimental analysis. With the improvement in computational techniques, the theoretical analysis gained special value to the design and development engineering, as well because it is very common that experimental analysis involves high costs. The experimental analysis is justified for the components of a complex systems, and it is possible that it be applied under orientation of computational modeling techniques. This kind of approach is common when the solutions for specific and complex problems results in theoretical solutions present low reliability because the high number of simplifications adopted.

Photoelasticity is an experimental technique for analysis and determination of stress/strain range of specific parts or engineering structures, specially of complex models. The photoelasticity is a powerful and efficient method of whole field analysis for plane or three-dimensional state. In the transmission photoelasticity, it is necessary to build transparent models with birefringency characteristics or optical anisotropy when loaded mechanically. For application of this technique, it is necessary to use an optical equipment called polariscope, which main feature is to work with polarized light. It give us the visualization of photoelastics parameters, in colored fringes, when it is used white light, or black and white fringes, when monochromatic light is used. This order fringe is associated with the stress state of the model.

Several authors have developed methods for treat the optical phenomenon of polarized light, like Theocaris P. S., Gdoutos E. E., 1979. The several forms of polarized light are defined by kinds of trajectory or curves that the final point of the light vector passes in the propagation wave. H. J. Menges, in 1940, and G.G. Stokes in 1852 proved that a defined kind of polarized light can be described by four parameters. This parameters are 4-elements of a vector, called Stokes vector. The Stokes parameters have dimension of intensity that can be operationally defined by intensity of emerging light, obtained by use of proper polarizer filters.

In this work, a software in Matlab® environment was developed applied to the acquisition and treatment of images of photoelastics models aiming at to get the orders of fringes of models submitted to a stress field. The images of the photoelastic models had been obtained by a connected digital camera directly to the polariscope. The technique that uses white light with elliptical polarization is presented, like developed by Yoneyama and Takashi (1998). In the determination of the orders of fringes, it was used a four points bending device to obtain a calibration table of a photoelastic model of a beam under bending conditions. With this, the main objective of the work was to automatize the process of reading, acquisition and treatment of the photoelastics parameters aiming at to improve the precision of the results and to facilitate the application of the transmission photoelasticity.

2. Plane transmission photoelasticity

The photoelasticity technique is based in the optical property of certain transparent plastic materials that presents different refraction indexes (or optical anisotropy) when submitted to a stress/strain condition (Dally and Riley, 1978).

The use of filters positioned between the observer, the light source and the model, give us the visualization of this phenomenon. These filters are part of the polariscope, equipment that polarizes the light that passes through it. The polarized light turns possible the observation of the stress by interpretation of the images which compose the optical parameters (Bernardes, Araújo and Neves, 2004).

2.1. The light and the optical relations in the photoelasticity

The electromagnetic theory of Maxwell shows that the light is an electromagnetic upset and it can be expressed like a normal vector to the propagation direction. The optical effects of the interest in photoelasticity can be described like a simple sine wave, flowing in positive direction of the z axes, like showed in the figure 1. Then, the light propagation in the z direction, when it is flowing from the origin can be represented like this:

$$E = f(z - ct) = A \cos \frac{2\pi}{\lambda}(z - ct) \quad (1)$$

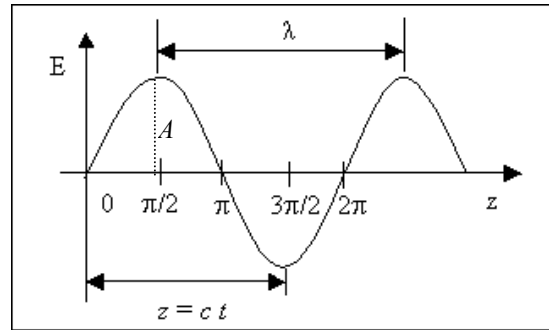


Figure 1. Amplitude of the vector light in function of the position in the propagation axis.

2.2. Polarized Light

The vibration associated with the light is perpendicular to the propagation direction. A light source emits waves contains transversal vibrations to the propagation direction. With the introduction of a polarizing filter (p) in the way of the light waves, only one of these components of vibrations will be transmitted (that parallel to the axis of polarization of the filter). This guided beam is called polarized light. If another polarizing filter (q) is placed in its trajectory, a complete extinguishing of the beam can be obtained if the axis of polarization of the two polariscopes are perpendicular between themselves. The white light, whose waves vibrate in all directions, when passing through the polarizers, is polarized on different lengths, i.e., in different colors. For example, the wavelength (λ) of 400 to the 450 nm corresponds to the violet light and the wavelength (λ) of 630 to the 700 nm corresponds to the red light.

The law of Brewster determines that the change of the refractive index is proportional to the difference between main deformations (Dally; Riley, 1978). By using this formularization the basic relation for the measure of deformation can be obtained, in terms of the principal stresses, called of stress-optic law, being given by:

$$\sigma_1 - \sigma_2 = \frac{NK\sigma}{b} \quad (2)$$

In The Equation (2) (K_σ) is the constant optic of the material, (N) is the fringe order and (b) the thickness of the model. When the two waves emerge from the model they are not simultaneous, due to the relative delay (δ), and if this model is between two polarizing lenses, the analyzer will only transmit a component of each of these waves, which will intervene themselves, and the intensity of resultant light, will be a function of the relative delay (δ) and the angle the axis of polarization of the analyzer and the direction of the principal stresses.

2.3. Photoelastic parameters

The interference caused by the phase among enters light beams propagating in the two main directions and the angle between the main directions and the axis of polarization of the polariscope give origin the two photoelastic parameters that can be measured.

The angle between the direction of polarization and main directions, is called parameter of the isoclinics, that are the geometric places of the points of the model that possess the same direction of the principal stresses, and these coincide with the directions of polarization of the polariscope. They are black curves (where the complete extinguishing of the light occurs) that appear in the analyzer of a plan polariscope and its value can be determined by turning the polarizer/analyzer set in relation to the model. They are necessary to localise the direction of the principal stresses.

The phase angle between the vectors light and the directions of the principal stresses, is called parameters of the isocromatics, and they are the geometric places of the points of the model, which have the same direction of the main stresses, and these coincide with the polarization directions of the polariscope. This parameter is easily identified in the circular polariscope, which has the property to eliminate the parameter of the isoclinics when the polariscope is adjusted to circulate polarized light. When the light source is white, the isocromatics are formed by luminous bands of different colorations depending on the fringe order (N), as shown in figure 2.

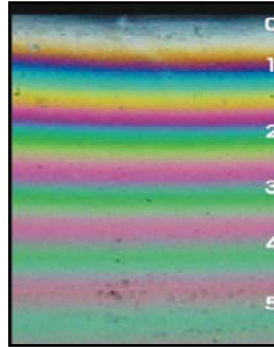


Figure 2. Isocromatic Fringe Orders.

3. Elliptical Polarized Light

Figure (3) presents the project of a typical polariscope formed by polarizing filters and delaying plates of one quarter forth of wave. In this case, the luminous rays spread along of z direction. Depending of the arrangement between the delaying plates and the polarized filters, polarized light (plain, circular, or elliptical) can be obtained. When a transparent model is stressed, a difference of phase occurs in the direction of the principal stresses between the vectors of emergent electric field of emerging light of the model cause by the birefringency effect. The emergent intensities of the light in the exit of a polarizing plan are given by:

$$I = I_0 \sin^2 \frac{\delta\pi}{\lambda} \sin^2 2(\varphi - \theta) \quad (3)$$

Where I_0 is the maximum value for the intensity of the emergent light, λ is the wave length, φ is the main direction of the double refraction, θ is the angle of polarization, δ is the delay of the linear phase (retardation) measured in nanometers. The linear retardation can be written in terms of the angle retardation (Δ) of the following form:

$$\delta = \frac{\Delta\lambda}{2\pi} = N\lambda \quad (4)$$

The equation of the intensity of the emergent light of a polariscope with a elliptically polarized light is derived by the calculations from Mueller, Theocaris P. S., Gdoutos E. E., 1979.

The Mueller matrixes for a linear polarizer P_θ with optic axis making an angle θ with the axis of reference and the delaying plate $R_\varphi(\Delta)$ with delay Δ , whose fast axis make an angle φ with the axis of reference are expressed by:

$$P_\theta = \frac{1}{2} \begin{bmatrix} 1 & \cos 2\theta & \sin 2\theta & 0 \\ \cos 2\theta & \cos^2 2\theta & \cos 2\theta \sin 2\theta & 0 \\ \sin 2\theta & \cos 2\theta \sin 2\theta & \sin^2 2\theta & 0 \\ 0 & 0 & 0 & 0 \end{bmatrix} \quad (5)$$

$$R_{\varphi} = \begin{bmatrix} 1 & 0 & 0 & 0 \\ 0 & \cos^2 2\varphi + \cos \Delta \sin^2 2\varphi & (1 - \cos \Delta) \cos 2\varphi \sin 2\varphi & -\sin \Delta \sin 2\varphi \\ 0 & (1 - \cos \Delta) \cos 2\varphi \sin 2\varphi & \cos \Delta \cos^2 2\varphi + \sin^2 2\varphi & \cos 2\varphi \sin \Delta \\ 0 & \sin \Delta \sin 2\varphi & -\cos 2\varphi \sin \Delta & \cos \Delta \end{bmatrix} \quad (6)$$

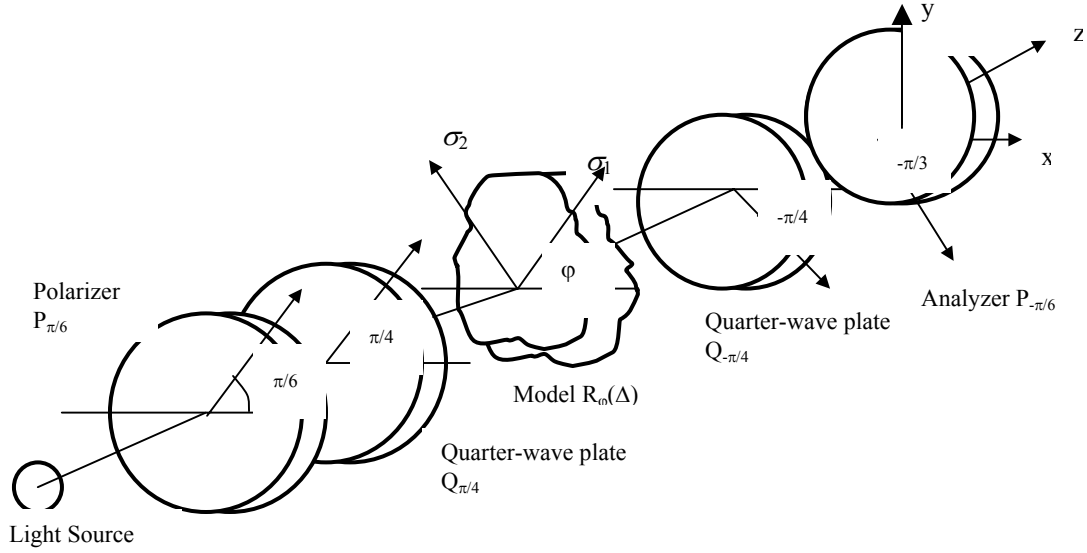


Figure 3. Model placed in a conventional polariscope.

The matrix of Mueller of the delaying wave plate can be obtained substituting $\Delta = \pi/2$ in the Eq. (6). In this work the axis of the polarizer and the analyzer make angles $\pi/6$ and $-\pi/3$ with relation to axis x and fixed axis of the delaying wave plates make angles $\pi/4$ and $-\pi/4$ with relation to axis x, respectively. The matrix of Mueller of the $P_{\pi/6}$ polarizer, $P_{-\pi/3}$ analyzer and wave plates of $Q_{\pi/4}$ and $Q_{-\pi/4}$, can be obtained substituting the respective angles in eqs. (5) e (6).

Once the wave plate is modulated for a specific wave length, the additional error in the delay of phase ε , is given by:

$$\varepsilon = \frac{\pi}{2} \left(\frac{\lambda_0}{\lambda} - 1 \right) \quad (7)$$

where λ is the wavelength of the used light and λ_0 is the specific wavelength for the delaying wave plate. The vector of Stokes (s) normalized of the non-polarized light emitted is defined as:

$$S = \begin{bmatrix} 1 \\ 0 \\ 0 \\ 0 \end{bmatrix} \quad (8)$$

Following the Mueller calculus, the vector of Stokes S' of the emerging light of the analyser is given by:

$$S' = [P_{-\pi/3} Q_{-\pi/4} R_{\varphi}(\Delta) Q_{\pi/4} P_{\pi/6}] S \quad (9)$$

So, from eqs. (5) to (9) it results:

$$S' = \frac{I}{64} \begin{bmatrix} 2(9 + \cos 2\varepsilon + 5 \cos 4\varphi + \cos 2\varepsilon + \cos 4\varphi + 4\sqrt{3} \sin \varepsilon \sin 4\varphi) \sin^2(\Delta/2) \\ (9 + \cos 2\varepsilon + 5 \cos 4\varphi + \cos 2\varepsilon + \cos 4\varphi + 4\sqrt{3} \sin \varepsilon \sin 4\varphi) \sin^2(\Delta/2) \\ (9\sqrt{3} + \sqrt{3} \cos \varepsilon + 5\sqrt{3} \cos 4\varphi + \sqrt{3} \cos 2\varepsilon \cos 4\varphi + 12 \sin \varepsilon \sin 4\varphi) \sin^2(\Delta/2) \\ 0 \end{bmatrix} \quad (10)$$

4. Automatic determination of fringe order

The light intensity emerging from the filter of the camera can be expressed as a function of a parcel of the intensity of the light defined for eq. (10) and of optical parameters of the acquired image, being given by:

$$I = I_0 \frac{1}{16} \frac{1}{\lambda_2 - \lambda_1} \int_{\lambda_1}^{\lambda_2} I_0 F_i \sin^2 \left(\frac{\delta \pi C_\lambda}{\lambda C_0} \right) (9 + \cos 2\varepsilon + 5 \cos 4\varphi + \cos 2\varepsilon \cos 4\varphi + 4\sqrt{3} \sin \varepsilon \sin 4\varphi) d\lambda \quad (11)$$

Where $i = r, g, b$ denote the colors red, green and blue, λ_{i1} and λ_{i2} are the minimum limits and maximum of the filters equipped in the camera and $F_i (= F_i(\lambda))$ they are spectral answers of the filters red, green and blue.

The error of the delaying wave plate (ε) and the dispersion of the double refringency are ignored on condition that the effect of these parameters are not very wide. Comparing the values of the intensity of the light in each point of the model analyzed with the corresponding values in one calibration table, which relates the order of the fringe with the values of the intensity of the light (Parameters RGB), the order of the fringe can be determined.

In the photoelastic technique proposal the fringe orders can be determined by two functions error, defined as:

$$E_j = (R_j - R_m)^2 + (G_j - G_m)^2 + (B_j - B_m)^2 \quad (12)$$

$$E_j = \left(\frac{R_j}{R_j + G_j + B_j} - \frac{R_m}{R_m + G_m + B_m} \right)^2 + \left(\frac{G_j}{R_j + G_j + B_j} - \frac{G_m}{R_m + G_m + B_m} \right)^2 + \left(\frac{B_j}{R_j + G_j + B_j} - \frac{B_m}{R_m + G_m + B_m} \right)^2 \quad (13)$$

Where R_m, G_m and B_m are values of the intensities of the digitalized lights I_r, I_g and I_b , for example the gray tones of the image in each point and R_j, G_j and B_j are also digitalized values obtained from the calibration table, respectively. The order of the fringe in each point can be determined through the index (j) that minimizes the function E_j error. The function error defined in eq. (13) is used as complement in the analysis due to the weakness of the intensity of the elliptical light. Therefore, the analysis of the fringe order can be executed by means of the two functions E_j error, evaluating itself the values of the indices (j) that minimize both functions and modulating the exits through the entire indices of the relative orders of fringe to each relative minimum.

If the variation of the order of the fringe in the table of the calibration is linear and first pixel of the calibration card is zero in the order of the fringe, the order of the N_j fringe corresponding to pixel (j) is given by:

$$N_j = N_m \frac{j}{j_m} \quad (14)$$

Where N_m is the maximal fringe order in the calibration table and j_m is the total of values archived in the calibration table.

5. Attainment of the photoelastic models

The methodology will be evaluated through a circular disk under constant compress load. This disk is made of photoelastic material. As shown in the previous section, it is necessary to use another phototoelastic model for the attainment of the calibration card. In this in case, the used model was a prismatic bar subjected to a four points bending. Figure 4 shows the dimensions of the models used in the analysis. The photoelastic models were produced from molds made of blue silica rubber. Figure 5 shows the silica molds used to cast the photoelastic models.

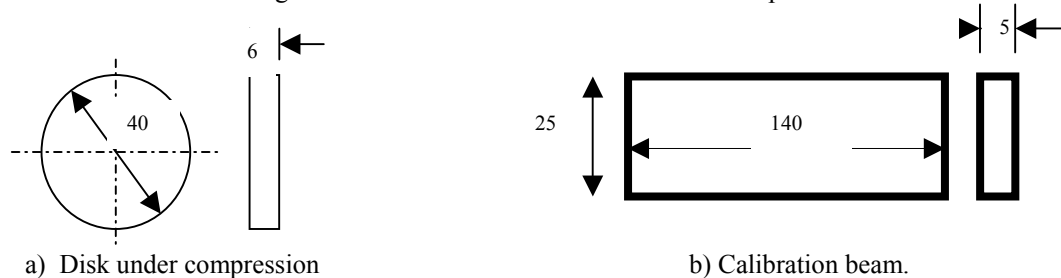


Figure 4. Dimensions of the analyzed models (mm).



Figure 5. Photoelasticity molds.

The photoelastic models were obtained from an epoxy-resin mixture and catalytic agent of the Polipox manufacturer. The ratio of a part in volume of the catalyser (Solution B) was used for two parts in volume of the resin (Solution A) as described in the work of Oliveira (2003). This resins was carefully mixed, approximately 15 minutes, trying to prevent the formation of bubbles. The fulfilling of the molds is made in the room temperature. To follow, they are left in a oven in the temperature of 25 °C during a period of 48 hours in order to complete the cure.

For the accomplishment of the experiments, the calibration model beam was placed in a polariscope developed in the Mechanical Project Laboratory (MPL) of the College of Mechanical Engineering, being located in a four-point compression load device. The load applied in the model was controlled by means of a load cell Kratos model of capacity 50 KN. The optical constant was obtained by a previous calibration process in the work of Araújo, Bernardes and Neves (2004), being of 0.26 N/mm. Despite the constant optics of the used material being low its optics reply is excellent, even for small applied load levels. Therefore, in the model of the calibration beam the load was 15 N generating fringes order of 3 in the model. Figure 6 shows the standard of fringes obtained in the calibration model.

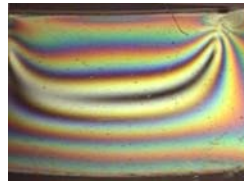


Figure 6. Standard of fringes in the central part of the calibration model using polarized elliptical light.

A circular disk loaded in diametral compression was placed in a polariscope with elliptical light for the validation of the technique proposed, under a 10 KN load. The images of the fringes values were acquired by a digital camera and transferred directly to the program, developed in Matlab environment. Figure 7 shows the standard of fringes obtained in the compressed disk. Figure 8 presents the schematic design for the technical development.

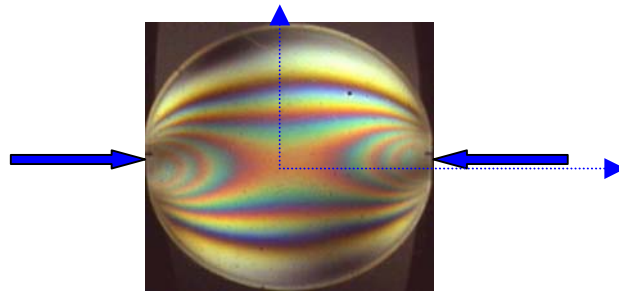


Figure 7. Standard of the photoelastic images for the disk under compression of 10 N.

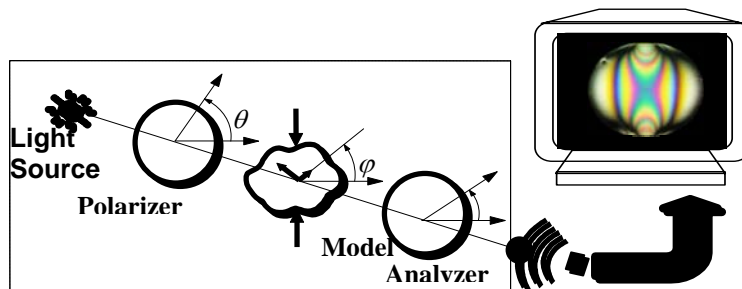


Figure 8 – Basic arrangement for using of the program.

6. Results

A load of 10 KN was applied in the disk monitored through a suitable load cell system. In this case the order of maximum fringe in the disk were approximately 7 as it shows figure 7. The results can be validated experimentally (manual reading) and also with the theory, since the analytical solution for disk model is known, Timoskenko, 1951. The calibration table used the RGB colors standard of the digital image of different fringe orders. In these cases, a valley in the image with gray tones represents a change in the entire order of fringe initiating with zero fringe. Developed software manipulates the images and the user defines the reading position appointed under the image of the calibration beam. To follow, the analysis band is defined between the bands maximum and of order zero that, in this case is the neutral line of the calibration beam (beam with bending pure). Figure 9 shows the standard of colors processed by the program and the relative curves to the gray tones and RGB parameters obtained. The calibration table is generated automatically and in the sequence, the image of the disk is loaded to be analyzed. The user then defines the point where he desires to get the fringe order and the program automatically calculates this value from the minimum energy proposed in this work.

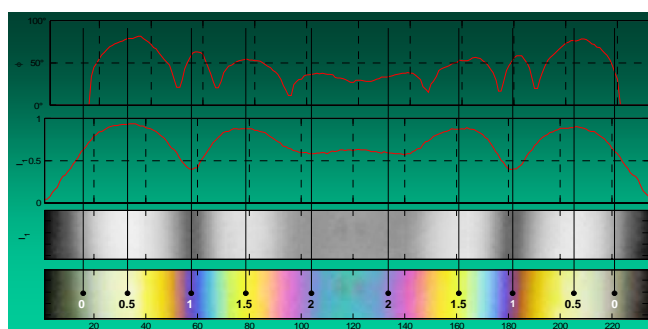


Figure 9 – Example of the graphic output generated by the program.

A points grid was created to evaluate the methodology in accordance with the figure 10. Table 1 shows the orders of fringe for the analyzed points in the disk under compression. The maximum shear stress (τ) can be obtained by :

$$\tau = \frac{\sigma_1 - \sigma_2}{2} = \frac{NK\sigma}{2b} \quad (15)$$

In the eq. (15) σ_1 and σ_2 are the principal stresses, with σ_1 being of tensile and σ_2 of compression. Figure 11 shows the calculated maximum shear stress in the models points analyzed, analytically and experimentally and by the software.

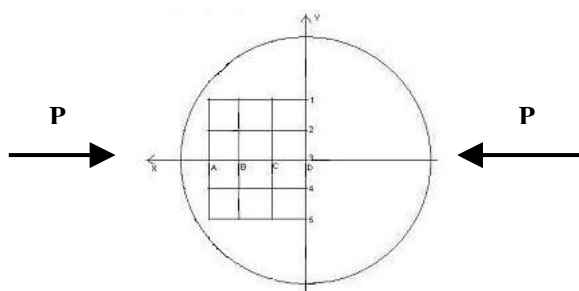


Figure 10. Point scheme in the photoelastic model analyzed.

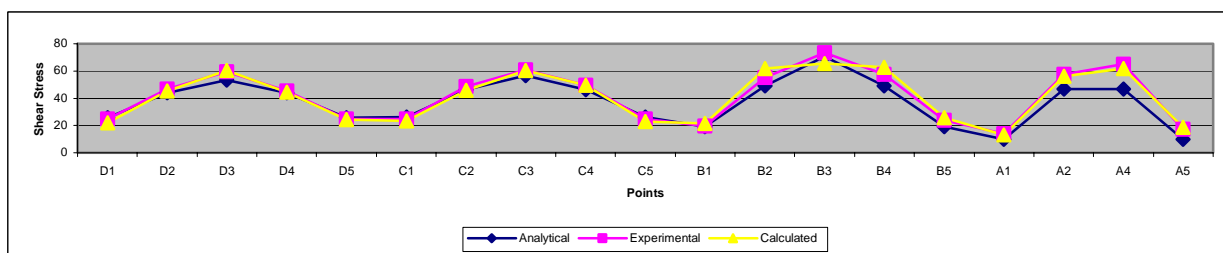


Figure 11. Maximum shear stress in Mpa for the points analyzed.

Table 1. Coordinates of the analyzed points.

Points		D1	D2	D3	D4	D5	C1	C2	C3	C4	C5	B1	B2	B3	B4	B5	A1	A2	A4	A5
Coord. (mm)	X	0	0	0	0	0	5	5	5	5	5	10	10	10	10	10	15	15	15	15
	Y	10	5	0	-5	-10	10	5	0	-5	-10	10	5	0	-5	-10	10	5	-5	-10

Table 2. Fringe orders (N) analytical, experimentally and for the program for the analyzed points.

N	D1	D2	D3	D4	D5	C1	C2	C3	C4	C5	B1	B2	B3	B4	B5	A1	A2	A4	A5
Analitical	1.18	2.04	2.45	2.04	1.18	1.21	2.14	2.61	2.14	1.21	0.89	2.27	3.26	2.27	0.89	0.46	2.17	2.17	0.46
Experim.	1.15	2.15	2.75	2.10	1.15	1.15	2.25	2.80	2.30	1.15	0.90	2.55	3.40	2.65	1.10	0.65	2.65	3.00	0.80
Calculated	1.01	2.09	2.78	2.06	1.13	1.09	2.12	2.78	2.28	1.06	0.99	2.60	3.02	2.50	1.09	0.60	2.59	2.86	0.87

The table 1 shows the coordinates of the analyzed model points (see fig. 10). The table 2 shows that the orders of fringe obtained by the method in the analyzed points are next to those obtained by the usual method (manual reading) and also through the analytical method. The manual reading was made following standards procedures of analysis of the fringes considering as 0.5 as being the maximum resolution in the fringe orders. For the analytical models a Matlab program was developed to calculate the stress in x,y directions which were been used to calculate the maximum shear stress. Using the eq. (15), the analytical orders of fringe can be calculated. Figure 11 shows that the behavior for the maximum shear stress was similar, differing in those points where the fringe order was of bigger order. As it was observed in the work of Yoneyama and Takashi (1998), due to its elliptical nature an attenuation in its intensity occurs. With this the method can be used with security in orders of maximum fringe of 3. For some noises in the photoelastic images were observed differences in some analyzed points.

7. Conclusions

The work presents a methodology for obtaining of the photoelastic parameters using polarized elliptical light. The validation of the technique proposed was made through a disk under compression load. All the photoelastic models and the experimental apparatus used and the evaluation of the methodology have been presented, with exception of the methodology for the determination of the principal stress directions. This is made through the numerical solution of a nonlinear equation obtained of the modeling with elliptical light shown in this work. This process is in progress, as well as refinements in the technique proposed, mainly, through the elimination of noises in the images. Due to its simplicity of implementation, the applied method can be used of advantageous and efficient form in the technique of photoelasticity. The photoelastic parameters of the model can be obtained automatically through the acquisition and processing of the image eliminating the inconveniences of a manual reading.

8. References

- Araújo, C. A. ; Neves, F. D.; Bernardes, S. R., 2004, "Stress analysis in dental implants using the photoelasticity technique". Proceedings of the 3th National Congress of Mechanical Engineering, Belém, Brazil.
- Dally, J. W. and Riley, W. F., 1978, "Experimental Stress Analysis". McGraw-Hill, Inc.
- Oliveira, E.J., 2003, "Material e técnica para análise fotoelástica plana da distribuição de tensões produzidas por implantes odontológicos." Dissertação (Mestrado em Reabilitação Oral) - Faculdade de Odontologia, Universidade Federal de Uberlândia, Uberlândia, Brazil.
- Pindera J. T., Cloud G., 1966 "On dispersion of birefringent of photoelastic materials" Exp. Mech., p470-80.
- Takashi M., Mawatari S., Toyoda Y., Kunio T., 1990, "A new computer aided system for photoelastic stress analysis with structure-driven type image processing." In Applied stress analysis, Elsevier Applied Sciences, London, p. 516-525.
- Timoshenko S. P., Goodier J. N., 1970, "Theory of elasticity", 3rd. ed. MacGraw-Hill Inc., New York.
- Theocaris P. S., Gdoutos E.E, 1979, "Matrix Theory of Photoelasticity" Proceedings of Springer-Verlag, New York.
- Yoneyama, S.; Takashi, M. 1998 "A new method for photoelastic fringe analysis from a single image using elliptically polarized white light", Optics and Lasers in Engineering, V 30, 441-459.

9. Responsibility notice

The authors are the only responsables for the printed material included in this paper.